Eur. Radiol. (2001) 11: 1807–1817
DOI 10.1007/s003300000728

A. Nömayr
M. Lell
R. Sweeney
W. Bautz
P. Lukas

MRI appearance of radiation-induced changes of normal cervical tissues

Received: 9 May 2000
Revised: 19 September 2000
Accepted: 20 September 2000
Published online: 18 January 2001

A. Nömayr (✉) · M. Lell · W. Bautz
Department of Diagnostic Radiology,
Friedrich Alexander University,
Maximiliansplatz 1,
91054 Erlangen-Nürnberg, Germany
E-mail: Anton.Noemayr@IDR.imed.uni-erlangen.de
Phone: +49-9131-8536066
Fax: +49-9131-8536068

R. Sweeney · P. Lukas
Department of Radiation Therapy,
Leopold Franzens University,
1090 Innsbruck, Austria

Abstract Irradiation causes specific MRI changes in anatomic morphology and signal intensity. To avoid misinterpretation, it is important to consider the potential radiation changes of normal tissue in MRI. The aim of this study was to describe the detected radiation effects on normal cervical tissues in MRI. Pretreatment and posttreatment MRI of 52 patients with primary neck tumors were evaluated retrospectively. The MR imaging was performed before initiating radiotherapy and at the end of the treatment period. Patients underwent follow-up studies within 24 months after the end of irradiation. Edema was the main radiation-induced effect. It was detected in the epiglottis, larynx, pharynx wall, retro- and parapharyngeal space, salivary glands, muscles, and subcutaneous tissue. In some cases the bone marrow of the mandible showed edema, due to osteonecrosis. We additionally detected fluid accumulation in the mastoid cells. Radiation caused volume reduction of the parotid gland, thickening of the pharynx wall, and fatty degeneration of bone marrow. Magnetic resonance imaging is an excellent method of depicting radiation-induced changes of normal tissue. Especially T2-weighted sequences allow the detection of even slight edema. It is important to be aware of the most common radiation-induced changes in MRI and to take them into account when assessing an examination.

Keywords MR · Radiation effects · Edema · Neck · Cervical tissues

Introduction

Irradiated tissue undergoes various changes. For example, patients complain about dysphagia and pain because of mucosal edema after irradiation in the neck region [1]. But without technical imaging, only a small part of all changes, such as erythema of the skin or oropharyngeal mucosa, are visible. Changes of tissue inside the body are only partly accessible to technical examinations, and, due to poor soft tissue contrast, detection of radiation injuries with most X-ray techniques, even CT, can be difficult. Magnetic resonance imaging is becoming increasingly important as a follow-up examination for previously irradiated tumors.

The main advantage of MRI is its excellent soft tissue contrast and the possibility of multiplanar imaging. Irradiation causes well-known defects in tissue which show characteristic changes in MRI. Mucosal edema causes a high signal on T2-weighted SE images and low signal in T1-weighted sequences. Radiation-induced replacement of bone marrow by fat results in hyperintense T1 signal intensity.

Another reason for using MRI is the excellent visualization of tissue with active and fast cell proliferation, such as malignant tumors. This tissue often shows hyperintense signal in T2 and hypointense signal intensity on T1-weighted sequences. It is difficult to distinguish between early postirradiation effects and tumors, because both may show similar signal intensity and contrast enhancement after i. v. gadolinium-DTPA. When assessing an MR examination after radiation therapy, it is important to know the potential radiation effects on normal tissue.

The focus of this article is to describe the effects of irradiation on normal cervical tissues in MRI.

Materials and methods

Patients

Pretreatment and posttreatment MRI of 52 patients (5 women and 47 men; age range 40–84 years, average age 58 years) with primary neck tumors were retrospectively evaluated. Tumors were located in the oro- and hypopharynx, the larynx, and the tongue/floor of the mouth. The tumor stages and locations are listed in Table 1.

All patients received two or three cycles of 6-MeV photon irradiation (first and second cycle 30 Gy, third cycle 10 Gy; total dose 60–70 Gy) and chemotherapy [10 mg/m^2 Mitomycine C i.v. and 1000 mg/m^2 5-Fluorouracil (5-FU) i.v.]. Irradiation was administered via two lateral neck fields, a supraclavicular field and a "boost" field on the tumor (third cycle 10 Gy). The dose was fractionated into 2 Gy per day (5 days/week). After a dose of 30 Gy, the dorsal part of the lateral neck field was irradiated with an electron beam (12 MeV).

Magnetic resonance imaging was performed with a 1.5-T whole-body unit (Gyroscan S 15, Philips, Eindhoven, The Netherlands) from July 1990 to October 1995. The examination protocol covered T1-weighted (TR 500 ms/TE 20 ms) and T2-weighted (TR 2200–3500 ms/TE 100 ms) conventional spin-echo (SE) sequences, inversion recovery (IR) sequences (TR 1400 ms/TE 30 ms/TI 120 ms) and T1-weighted SE images after gadolinium-DTPA i.v. (0.1 mmol/kg).

Slice thickness was 6 mm with an interslice gap of 10%. The field of view (FOV) was 250 mm with a matrix size of 256 × 256. A head-neck coil was used to improve spatial resolution. Images were obtained from the base of the skull to the level of the sternoclavicular joint in axial and sagittal or coronal planes.

The MR examinations were performed before initiating therapy and then within 2 weeks of the end of each irradiation cycle (after a dose of 30, 60, and 70 Gy). Posttreatment examinations were performed within 6–24 weeks, 6–12 months, and 12–24 months after irradiation. These posttreatment examinations were compared with the MRI studies following the second (60 Gy) or third irradiation cycle (70 Gy), but not all patients were examined in these time intervals and not all anatomic regions were irradiated with the same dose due to different field borders, and often not all anatomic regions were included in the scan (retrospective evaluation). Therefore, evaluating different anatomic structures at different times resulted in differing patient numbers. To avoid misinterpreting surgery-induced effects with those caused by radiation, examinations performed on patients who had received surgery (n = 16) were not included in the assessment.

In evaluating the MRI studies, images of 1 patient were compared with examinations of the same patient at different times, considering changes in signal intensity and anatomic morphology. The evaluation was done retrospectively by three readers in consensus (A.N., M.L., P.L.).

All measurements were done retrospectively by one reader (A.N.).

Parotid gland

In 25 cases the volume of the parotid gland was measured before and after irradiation. The volume was determined by measuring the gland surface of each slice (computer assisted). To evaluate the approximate gland volume, the summation of the gland surfaces of all slices was multiplied by the summation of slice thickness and slice gap. The volume was compared with the follow-up examinations of the same patient. The gland volume before starting irradiation was set to 100%. Measurement error was 5.6% (evaluated by 30 measurements of one gland).

Table 1 Fifty-two patients with squamous cell carcinomas of the neck. Tumor locations and tumor stages according to the TNM classification [32]. M-staging was excluded. *G* histopathological tumor grading (G1–G3)

Oropharynx	Tongue/floor of the mouth	Hypopharynx	Larynx
T3, N0, G3	T3, N1, G2	T4, N2, G2 × 7	T2, N2, G2
T3, N2, G2	T4, N0, G2	T4, N2, Gx	T3, N0, G3
T3, N2, G3	T4, N1, G1	T4, N2, G3 × 7	T4, N2, G3 × 3
T3, N3, G3	T4, N1, G2 × 3	T4, N3, G3 × 5	
T4, N0, G3	T4, N2, G2 × 6		
T4, N1, G2			
T4, N2, G2 × 9			

Pharynx wall/retropharyngeal space

In 20 cases the anterior–posterior thickness of pharyngeal wall and retropharyngeal space at the level of the tip of the epiglottis was measured with calipers. Due to irradiation, it was often not possible to distinguish between pharynx wall and retropharyngeal space, so they were measured together. The measurement error was 4% (evaluated by 30 measurements of the diameter of one pharynx wall/retropharyngeal space).

Results

Reactive changes occurred in the epiglottis, larynx, pharynx wall, retro- and parapharyngeal space, salivary glands, muscles, mastoid cells, subcutaneous tissue and bone marrow. Intensity of these effects depended on administered dose and time elapsed after irradiation.

In general, the epiglottis was thickened (hyperintense signal intensity on T2-weighted SE MR images). This was due to accumulation of fluid in the tissue (edema; Figs. 1, 2; Table 2). Edema was visible in 85% of all cases (70 Gy). In follow-up MR studies, edema decreased (Table 2). Radiation therapy (70 Gy) caused thickening and hyperintense signal intensity on T2-weighted sequences (edema) of larynx mucosa (80%; Fig. 2; Table 2). In follow-up studies a decrease in signal intensity (T2-weighted image) and thickening of the mucosa was visible (Table 2). Edema of subcutaneous tissue occurred in 94% of patients treated with 70 Gy (Figs. 1, 2; Table 2). Physical examination showed thickening of subcutaneous tissue (especially in the submandibular area). Six to 24 weeks after the end of irradiation, signal intensity (T2-weighted sequence) was stronger than that of the post-70 Gy MRI (Table 2).

Irradiation caused a signal elevation on T2-weighted images and a hypointense signal intensity on T1-weighted sequences (edema; Fig. 1, 3, 2, 10) in pharynx wall and retropharyngeal space. Contrast-enhanced T1-

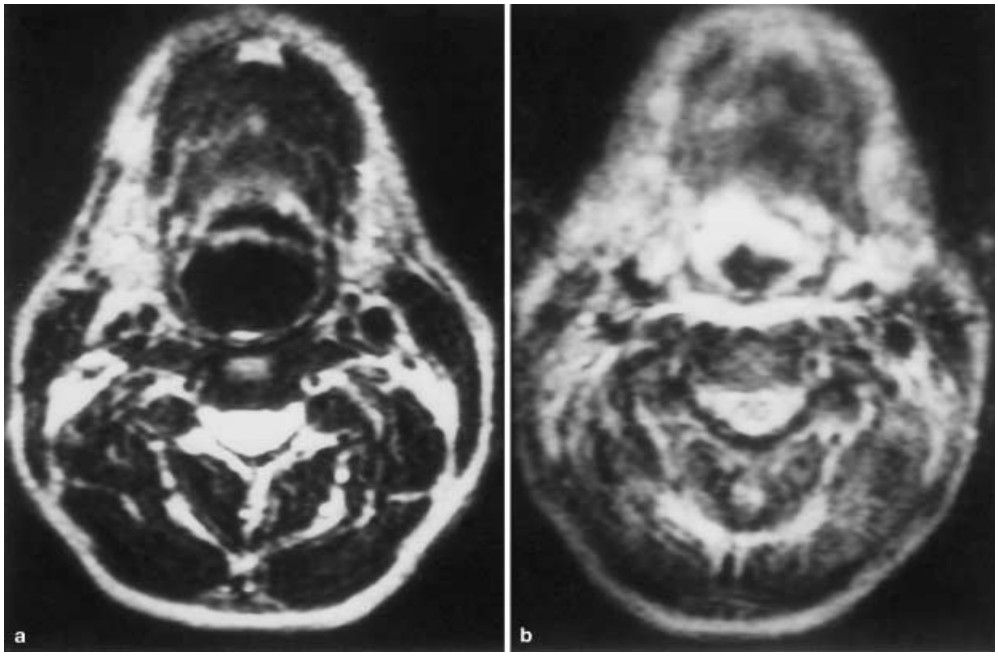

Fig. 1 a, b T2-weighted spin-echo (SE) MRI (TR 3500 ms, TE 100 ms) **a** before and **b** after irradiation (70 Gy; squamous cell carcinoma of the tongue; T4, N1, G2). After irradiation: Epiglottis edema, edema of pharynx wall and retro-/parapharyngeal space, subcutaneous edema. Thickening of epiglottis, pharynx wall, and retropharyngeal space

weighted images (gadolinium-DTPA i.v.) exhibited enhancement and thickening of pharynx wall and retropharyngeal space (Fig. 3) in 93% of all cases (Fig. 2; Table 2).

After therapy, these effects decreased slowly (Table 2). Radiation-induced edema of the anterior larynx muscles (Fig. 4) was detected in 2 patients following irradiation (70 Gy). No further MRI studies were performed. In all cases, the caudal mastoid cells were within the lateral fields (60 Gy). No "boost" (third cycle) was applied on the mastoid cells. In 47% of the cases, mastoid cells showed a signal elevation on T2-weighted images post irradiation (70 Gy; Figs. 5, 2; Table 2), without enhancement after Gd-DTPA i.v. (T1-weighted sequence), due to accumulation of fluid in the mastoid cells. Additional irradiation (30 Gy) in the neck region, not including the mastoid, caused increased signal intensity (T2-weighted sequence) in 3 of 6 patients. Six months after the end of therapy, signal intensity decreased in all cases (Table 2).

Parotid and submandibular glands were irradiated with a dose of 60–70 Gy. In 22% (parotid gland) and

Table 2 Number of patients (x) with radiation-induced changes in relation to all patients (n) irradiated in the particular anatomic region (x of n). Increase/decrease/constant: evaluation of the radiation-induced effect compared with the initial posttherapy MR examination (70 Gy)

Dose and time after irradiation						
Change	30 Gy	60 Gy	70 Gy	6–24 weeks after irradiation (70 Gy)	6–12 months after irradiation (70 Gy)	> 1 year after irradiation (70 Gy)
Epiglottis edema	10 of 21	6 of 12	11 of 13	7 of 7 (constant)	1 of 3 (constant)	1 of 4 (decrease)
Larynx edema	7 of 21	8 of 14	8 of 10	4 of 5 (constant)	4 of 6 (constant)	4 of 6 (decrease)
Edema of pharynx wall, retro- and parapharyngeal space	14 of 24	13 of 14	13 of 14	11 of 11 (constant)	5 of 6 (decrease)	5 of 6 (decrease)
Parotid gland edema	3 of 24	2 of 14	2 of 9	1 of 5 (decrease)	0 of 5	0 of 5
Submandibular gland edema	3 of 24	4 of 14	4 of 13	2 of 8 (decrease)	0 of 3	–
Fluid in mastoid cells	3 of 25	2 of 15	7 of 15	3 of 11 (decrease)	–	–
Fatty degeneration of bone marrow	22 of 35	35 of 35	35 of 35	22 of 22 (increase)	8 of 8 (constant)	7 of 7 (constant)
Subcutaneous edema	11 of 29	12 of 16	17 of 18	11 of 11 (increase)	3 of 3 (constant)	5 of 6 (decrease)

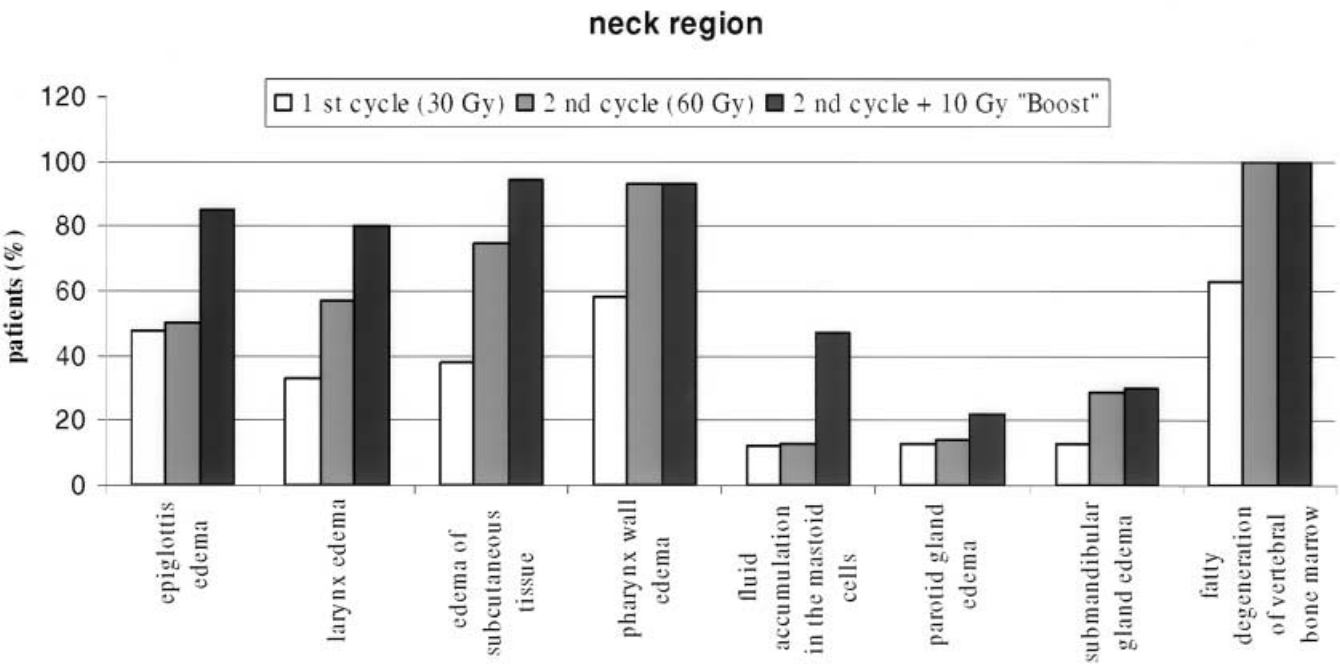

Fig. 2 Radiation-induced changes in the neck region. Number of patients (%) with radiation-induced changes in relation to irradiation dose

31 % (submandibular gland) hyperintense signal intensity (edema) was visible after irradiation on T2-weighted images (Fig. 2; Table 2). Parotid gland volume decreased after irradiation (Figs. 6, 7, 8). After therapy, the signal intensity (T2-weighted sequence) declined while the reduction in volume persisted (Fig. 8). Compared with posttherapy MR examinations (70 Gy), later follow-up studies did not show further significant volume reduction (Fig. 8). The vertebral bodies (neck) were irradiated with a total dose of 30–35 Gy. The most common effect of irradiation on vertebral bone marrow was a signal elevation on T1-weighted images (accompanied by an intermediate signal intensity on T2-weighted images), due to fatty degeneration of bone marrow (Fig. 2). After the first cycle (30 Gy), 63 % of all

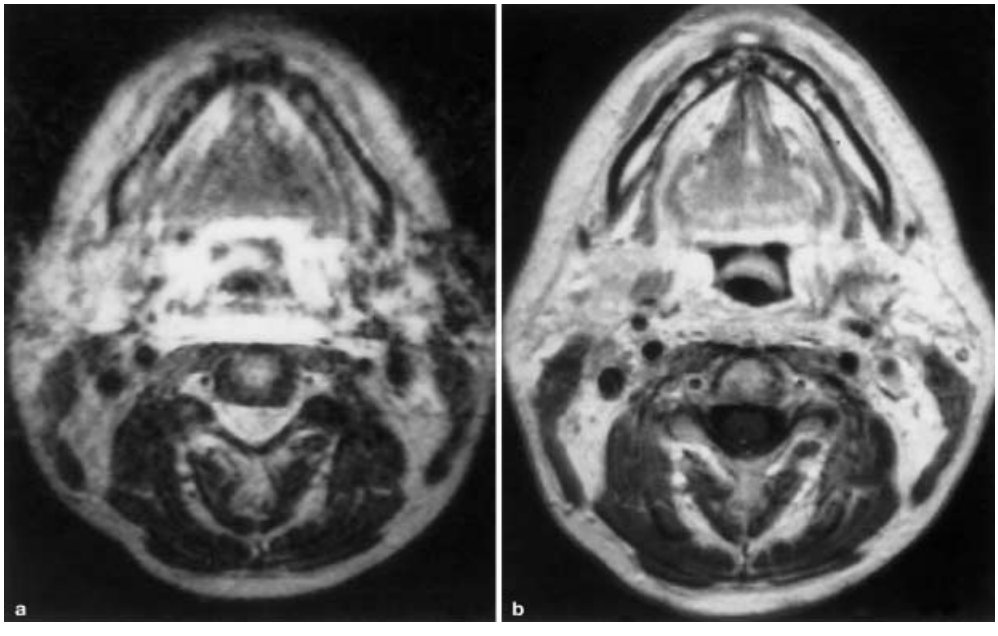

Fig. 3 **a** T2-weighted SE (TR 3500 ms, TE 100 ms) and **b** T1-weighted SE (gadolinium-DTPA i. v., TR 500 ms, TE 20 ms) MRI 2 months after irradiation (70 Gy; squamous cell carcinoma of the tongue; T4, N2 G2). Thickening of epiglottis, pharynx wall, and retropharyngeal space with contrast enhancement

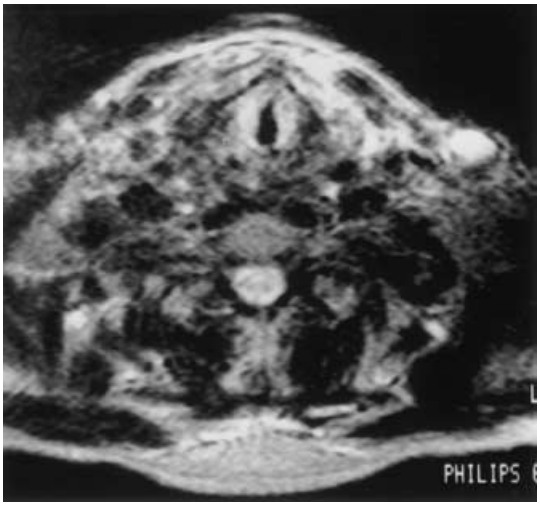

Fig. 4 T2-weighted SE MRI (TR 3500 ms, TE 100 ms) 6 months after irradiation (70 Gy) and 5 months after additional irradiation (30 Gy) (squamous cell carcinoma of the hypopharynx; T4, N2, G3). Edema of the ventral neck muscles with hyperintense signal intensity

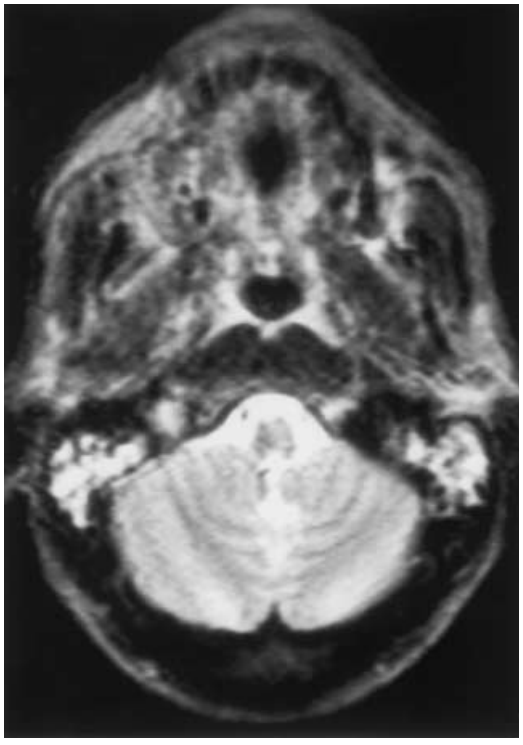

Fig. 5 T2-weighted SE MRI (TR 3500 ms, TE 100 ms) 5 weeks after irradiation (70 Gy; squamous cell carcinoma of the hypopharynx; T4, N2, G2). Fluid accumulation in the mastoid cells with hyperintense signal intensity

patients showed this effect. After 60 Gy, this was visible in all cases (Table 2). Follow-up MR examinations 6–24 weeks after therapy showed an increased signal intensity on T1-weighted images compared with the posttherapy MRI (Table 2). Replenishment of blood-building marrow with decreasing signal intensity (T1-weighted sequence) was not visible following therapy. The mandibles were within the lateral fields and received 60 Gy. In 11 cases the "boost" (additional 10 Gy on the tumor) included different parts of the mandible. As a result of fluid accumulation in bone marrow (edema), parts of the mandibles showed hyperintense signal intensity (T2-weighted sequence) accompanied by hypointense signal on T1-weighted images in 5 cases (Fig. 9). This effect occurred 11–43 months after irradiation (60 Gy). No follow-up studies were performed. Signal intensity (T1-weighted images) of mandible bone marrow preceding irradiation was hyperintense (fat) in all other cases.

Residual/recurrent tumor

A localized, expansive mass with intermediate signal intensity on T1, marked enhancement on T1 after the application of Gd-DTPA, and hyperintensity on T2 was suspicious for a residual or recurrent tumor.

Regarding MRI examinations subsequent (0–2 weeks) to the end of therapy (60/70 Gy), in 17 of 35 cases a residual mass was still visible in the tumor region with contrast enhancement (T1) after Gd-DTPA i.v. and hyperintense signal on T2-weighted sequences. Histological examinations were performed in all of these cases. In 9 patients inflammatory reaction was found. Magnetic resonance imaging could not differentiate between residual tumor and irradiation-induced inflammatory reaction of the tumor region, due to equal signal characteristics (hyperintense signal on the T2-weighted sequence and contrast enhancement on T1-weighted images after Gd-DTPA i.v.). Two patients showed progressive tumor size after 60 Gy, which was interpreted as tumor non-response (histologically proven).

The posttreatment MRI examinations (6 weeks to 2 years after therapy) were compared with the examinations done within 0–2 weeks after the end of therapy (60/70 Gy). Twenty-two patients had a posttreatment MRI examination 6–24 weeks after the end of the therapy. Seven patients (7 of 22) showed a residual mass, with hyperintense signal on the T2-weighted sequence and contrast enhancement (T1) after Gd-DTPA i.v. Malignant tumor cells were found in two 2 cases. In 5 cases the histological examination found inflammatory reaction. Magnetic resonance imaging could not differentiate between malignant tumor and inflammatory reaction.

Eight patients received a posttreatment MRI examination 6–12 months after therapy: 4 of 8 patients had a residual mass in the former tumor region. In 2 cases the

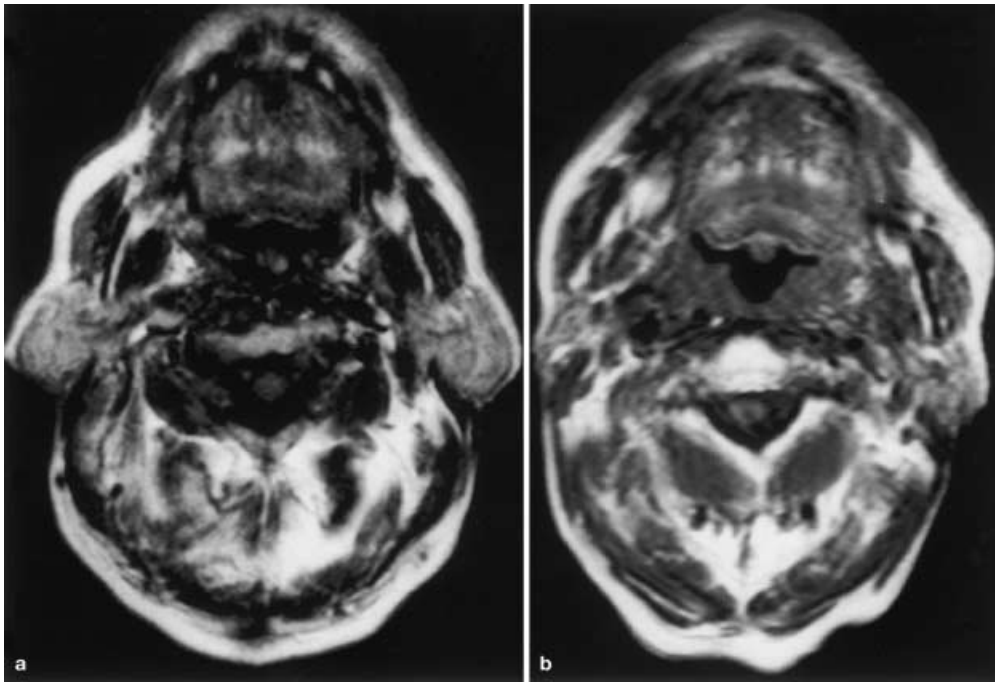

Fig. 6 a T1-weighted SE MRI (TR 500 ms, TE 20 ms) a before and b 2 years after irradiation (70 Gy; squamous cell carcinoma of the tongue root; T4, N2, G2). Volume reduction of the parotid glands (~ 50 %)

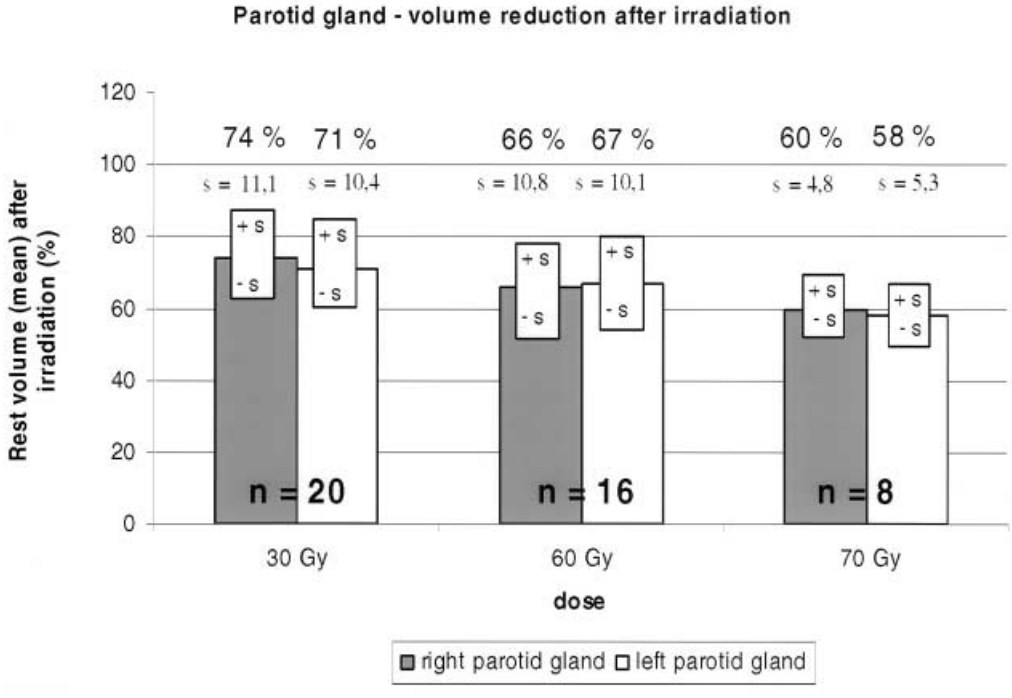

Fig. 7 Radiation-induced mean volume reduction (%) of the parotid gland (volume before therapy = 100 %, ± one standard deviation). *n* number of cases where gland volume was measured

space-occupying tissue showed reduced signal on the T2-weighted sequence with low contrast enhancement (T1) after Gd-DTPA i. v. The histological examination found fibrosis. The remaining 2 patients showed a residual mass with hyperintense signal intensity on T2-weighted sequences and significant contrast enhancement (T1) after Gd DTPA i. v. The histological examination revealed malignant tumor cells in 1 case and a hypervascular scar with inflammatory reaction in the other case.

Seven patients underwent MRI within 12–24 months after therapy. Four patients still showed space-occupy-

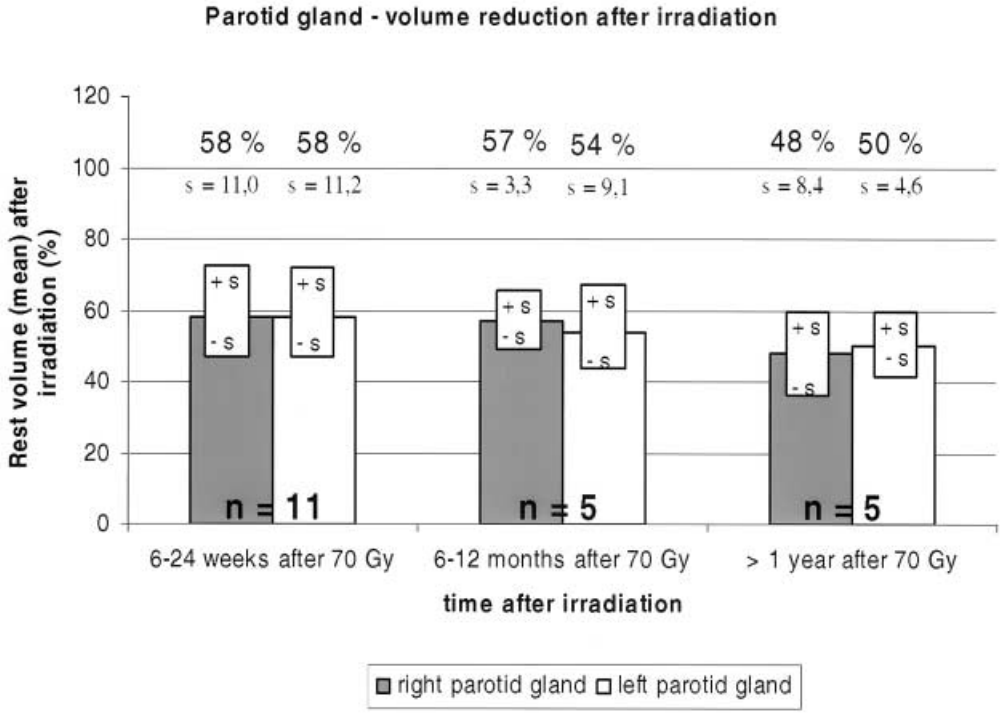

Fig. 8 Radiation-induced mean volume reduction (%) of the parotid gland (volume before therapy = 100 %, ± one standard deviation). *n* number of cases where gland volume was measured

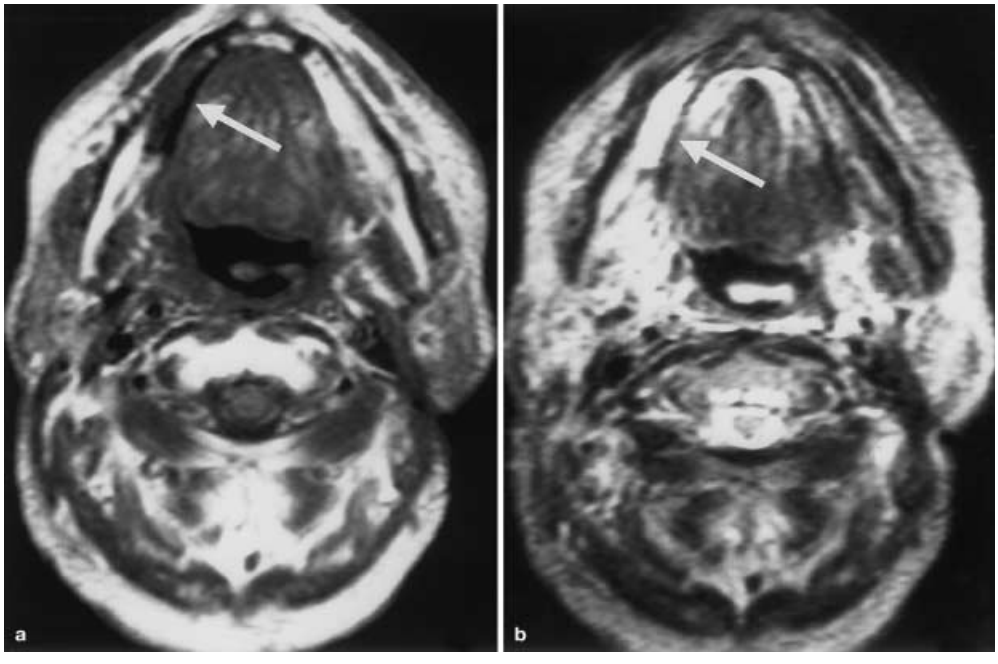

Fig. 9 **a** T1-weighted spin-echo (TR 500 ms, TE 20 ms) and **b** T2-weighted SE MRI (TR 3500 ms, TE 100 ms) 11 months after irradiation (70 Gy; squamous cell carcinoma of the (left) oropharynx; T3, N2, G3). Bone marrow edema of the (right) mandible (osteonecrosis, histologically proven) with hypointense signal in a and elevated signal intensity in **b**

ing tissue in the former tumor region. In 3 cases this tissue was hypointense on T2-weighted images without significant contrast enhancement (T1) after Gd-DTPA i.v. These signal characteristics were interpreted as fibrosis. In two of these cases, however, fibrosis had been found on previous histological examinations (6–12 months after the end of therapy). One patient had a localized, expansive mass which showed hyperintense signal on the T2-weighted sequence and contrast enhancement after Gd-DTPA i.v., which was interpreted as recurrent tumor (histologically proven).

Discussion

The first visible effect of radiation on normal tissue was edema, presenting as hyperintense signal intensity on T2-weighted sequences and hypointense signal intensity on T1-weighted images. Contrast-enhanced MR studies (gadolinium-DTPA i.v.) showed an elevated signal intensity in the areas of edema (excluding the mastoid cells). Calcaterra et al. [2] and Manara and Mira [3] described the histopathological findings of this interstitial edema in an irradiated larynx. The reason for this effect is early damage of blood and lymph vessel endothelium with increasing permeability to fluid. After irradiation, beginning fibrosis of connective tissue and small vessels is seen, leading to reduced lymph transport with constant interstitial fluid accumulation (= edema). This effect may decrease over time, due to revascularization [3].

Epiglottis

In 85 % of all cases in this study, epiglottic edema occurred following irradiation (70 Gy). This effect was dose dependent (Fig. 2). The examinations performed within 6–12 months after therapy showed decreasing edema. That is in accordance with the histopathological findings of Manara and Mira [3]. Using CT and a comparable dose Mukherji et al. [4] reported thickening of the epiglottis which they interpreted as edema following irradiation in 63 % of all cases. The possible explanation for the difference (63 vs 85 %) may be the better soft tissue contrast in MRI, allowing edema to be detected before thickening of the epiglottis is visible. Another reason may be that all patients in our study underwent chemotherapy.

Larynx

Laryngeal edema is caused by damage to small blood and lymph vessels in the mucosa and the perichondral tissue [2]. Since chondral tissue is relatively resistant to radiation, changes are rarely visible [2]. The incidence of laryngeal edema depended on dose. Using CT, Mukherji et al. [4] found radiation-induced thickening of vocal cords and laryngeal mucosa which is comparable to our results.

Retro-/parapharyngeal space

Following a dose of 60–70 Gy, edema of pharyngeal wall and the retro-/parapharyngeal space occurred in most cases (Fig. 1, 3, 2, 10; Table 2). This effect was dose dependent (Fig. 2, 10; Table 2). The pharynx wall consists of mucosa and muscularis. The retro- and parapharyngeal space is located cranially from the thyroid cartilage between the longus colli muscle and the pharynx wall. Mukherji et al. [4] found a thickening of pharynx wall and retropharyngeal space on CT. We also observed a dose dependent thickening of these structures (tissue edema; Fig. 2). This effect began to diminish 12 months after completion of therapy.

Subcutaneous tissue

Subcutaneous edema following irradiation was very common and dose dependent. Examinations performed 6–24 weeks after therapy showed increasing T2 signal intensity in 50 % of all cases Table 2. This could be a delayed effect, due to damaged small lymph vessels [3]. Our follow-up MR studies showed decreasing edema. Mukherji et al. [4] found thickening of the subcutaneous tissue on CT (= edema) in 63 % of all cases. In the current study, edema occurred more often. This might again be due to better tissue contrast and fluid detection using MRI. Another reason might be chemotherapy in our study.

Muscles

Muscle edema was rarely observed following irradiation in the neck region (2 cases). In electron microscopy studies on rabbit tissue, Khan [7] found muscle edema 12 h after irradiation. Sovic et al. [9] reported edema of pelvic muscles in MRI following irradiation.

Whereas fibrosis or fatty muscle degeneration were not detectable in this study, Manara and Mira [3] did detect muscle fibrosis and fatty degeneration in histopathological examinations.

Mastoid cells

The tympanum is connected with the nasopharynx by the eustachian tube and normal mastoid cells are pneumatized and lined with mucosa. Hyperintense T2 signal in mastoid cells occurred in 12 % after irradiation with a dose of 30 or 60 Gy (mastoid cells included in the radiation field, posttherapy MRI). Additional "boost" therapy (third cycle 10 Gy) on the tumor (mastoid cells were not included in the "boost" field) led to increasing signal intensity of mastoid cells on T2-weighted images. Three of the six patients who underwent additional irradiation (30 Gy) of the neck, not including the mastoid cells, showed a further increase of signal intensity on T2-weighted images (elevated signal intensity on T2-weighted sequences was already visible after irradiation with 70 Gy), although mastoid cells were not included in

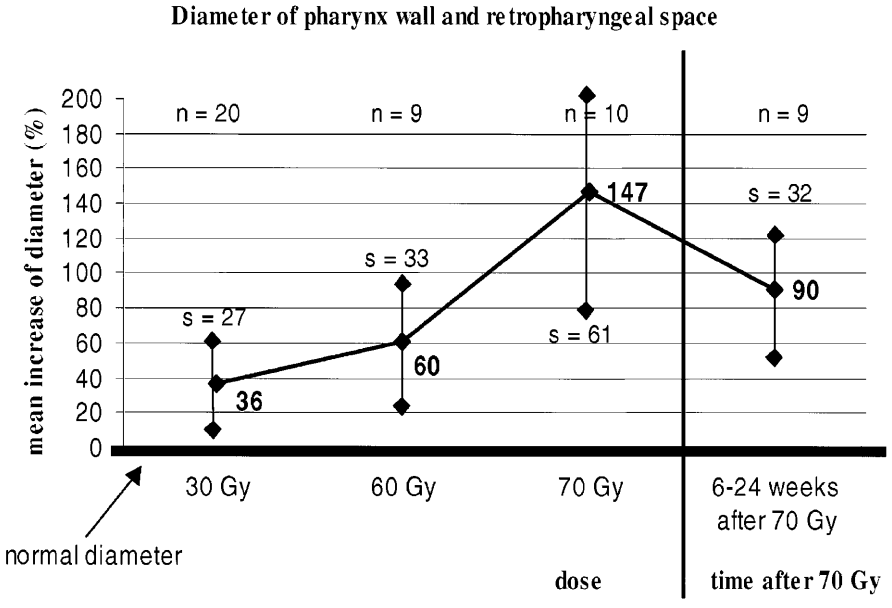

Fig. 10 Radiation-induced thickening of pharynx wall and retropharyngeal space. Mean increase of the diameter (percent ± one standard deviation in relation to irradiation dose and time after irradiation (70 Gy). Measurement with calipers: $n = 20$ (after 30 Gy); $n = 9$ (after 60 Gy); $n = 10$ (after 70 Gy); and $n = 9$ (6–24 weeks after 70 Gy)

this new field. Since the mastoid cells did not enhance after i.v. Gd-DTPA, this effect could be a result of fluid accumulation. Irradiation of mastoid cell mucosa might not be the only reason for this effect. Irradiation of neck tissue causes damage to lymph vessels and might reduce the function of the eustachian tube with resulting fluid accumulation in the mastoid cells. Maier et al. [10] reported reduced tube function with less aeration of the middle ear following irradiation, attributing this to damaged lymph vessels with decreased lymph flow. Fluid accumulation in mastoid cells may be related to reduced tube function, decreased lymph flow, and irradiation of mastoid cell mucosa. Ohashi et al. [11] also found reduced tube function after irradiation. Six to 24 weeks after irradiation, we found decreasing signal intensity in T2-weighted images. Maier et al. [10] found tube function to improve 6 months after the end of irradiation.

Salivary glands

All patients showed volume reduction of the parotid gland. Stephens et al. [12] reported reduced gland parenchyma attributable to the loss of serous cells. This effect was more pronounced in the parotid gland than in the submandibular gland, possibly due to the higher number of serous cells of the parotid gland [12, 13, 14, 15]. In addition, Vissink et al. [16] found a higher radiation sensitivity of the parotid gland compared with the submandibular gland. In our study parotid gland volume was reduced by an average of 26% following 30 Gy. After 70 Gy, volume was reduced by approximately 40%. Nagler et al. [15] found dose-dependent weight reduction of salivary glands. In our study no restitution of parotid gland volume was detected in the follow-up studies after irradiation with 60–70 Gy. Franzen et al. [17] reported a recovery of salivary gland function after doses under 52 Gy. After 64 Gy and more, no restitution was detected. After irradiation with 70 Gy, salivary gland edema, corresponding to sialadenitis, was detected in 2 of 9 cases (parotid gland) and in 4 of 13 cases (submandibular gland).

Bone marrow

Bone marrow edema of the mandible might be due to osteonecrosis. In our study, bone marrow edema of the mandible occurred in 5 cases, representing osteonecrosis (histologically proven). Knospe et al. [19] and Aitasalo [20] found destruction of hematopoetic marrow, osteoclasts, osteoblasts, and an obliterative endangitis of small vessels with an increase of interstitial fluid. Frequently, infection of the parodontium is one cause [21, 22]. Scherer and Sack stated that radiation induced reduced blood supply of the mandible causes immunodeficiency [8], making it susceptible to infection. We observed 5 cases of osteonecrosis (histologically proven) of the mandible with elevated signal intensity on a T2-weighted sequence, representing edema. Schratter-Sehn et al. [23] detected osteonecrosis of the mandible in 5–8% (60 Gy). Bachmann and Rössler [24] found osteonecrosis in 6% of all cases within a variable time interval (3 months to 4 years) after irradiation. This effect occurred less often after 40 than after 60 Gy [24]. After irradiation with 60 Gy, fatty degeneration of vertebral bone marrow was reported in all cases (in our

study, total dose on vertebral bodies was 30–35 Gy). Compared with the posttreatment MRI, the follow-up MR studies, performed 6 weeks to 1 year after irradiation, showed increasing T1 signal intensity in 50 % of all cases (due to increasing fatty degeneration of bone marrow). No regeneration of bone marrow signal intensity was detectable. Knospe et al. [19] and Aitasalo [20] described radiation-induced replacement of hematopoetic marrow with fat. Kauczor et al. [25], Dietl et al. [26], and Parmentier et al. [27] also reported fatty degeneration of bone marrow after irradiation. After doses over 30 Gy, no regeneration of bone marrow was visible [26].

Residual/recurrent tumor

Irradiation caused edema with intensified permeability of vessel endothel and a fibrous-inflammatory reaction [2, 3]. These irradiation-induced effects showed tumor-like signal intensities on MRI (hyperintense signal intensity on T2/T1 after Gd-DTPA i.v.) [28, 29, 30]; therefore, it was difficult to differentiate between residual/recurrent tumor and fibrous-inflammatory reaction on MRI, especially in examinations done within 6 months after irradiation with intensive edema of the tumor region and the surrounding tissue. This edema obscured the borders of the tumor, led to overestimation of the tumor size, and reduced the contrast between tumor and surrounding tissue. The detection of a small residual/recurrent tumor could be hampered by the inflammatory reaction. The inflammatory edema could be misinterpreted as malignant tumor, due to equal signal characteristics in MRI. The intensified permeability of altered endothels (irradiation) led to enhancement after the application of Gd-DTPA i.v., which could not be differentiated from tumor enhancement. Several authors reported difficulties in the differentiation between inflammatory reaction and residual tumor using MRI [28, 29, 30]. Engelbrecht et al. found MRI to be superior to CT in this problem [28]. In our study the posttreatment MRI examinations up to 6 months after the end of therapy did not allow a differentiation between residual tumor and inflammatory reaction of the former tumor region.

Later MRI examinations (6–24 months after therapy) improved the detection of recurrent or residual tumors, due to a good contrast between tumor (hyperintense signal on T2/T1 Gd-DTPA) and the surrounding "normal" tissue. This was due to regressive inflammatory edema of the surrounding tissue. The regression could be explained by capillary and lymphatic neogenesis and increasing fibrous reaction with low signal on T2- and T1-weighted sequences [3]; therefore, Sugimura et al. recommended posttreatment MRI examinations not earlier than 4 months after therapy, to improve the detection of residual/recurrent tumors [31]. The differentiation between residual/recurrent tumors and hypervascular scars of the former tumor region is still difficult, however. Hypervascular scars with hyperintense signal intensity on T2-weighted images and contrast enhancement after the application of Gd-DTPA i.v. can persist over years and only the reduction of size in regular follow-up examinations can prove the benign character of the lesion [30].

Conclusion

To accurately interpret MRI studies of patients who previously underwent radiation therapy due to malignancy, knowledge of expected radiation-induced changes in MRI is paramount. Understanding of these alterations and their evolution may prevent misinterpreting such reactive changes as residual or recurrent tumor.

References

1. Grant B, Fletcher G (1966) Analysis of complications following megavoltage therapy for squamous cell carcinoma of the tonsillar area. AJR 96: 28–36
2. Calcaterra TC, Stern F, Ward PH (1972) Dilemma of delayed radiation injury of the larynx. Ann Otol 81: 501–507
3. Manara G, Mira E (1968) Histological changes of the human larynx irradiated with various technical therapeutic methods. Arch Ital Otol 79: 596–635 [in Italian]
4. Mukherji SK, Mancuso A, Kotzur I, Mendenhall W, Kubilis P, Tart R, Lee W, Freeman D (1994) Radiologic appearance of the irradiated larynx. Part I. Expected changes. Radiology 193: 141–148
5. Quillin SP, Balfe D, Glick S (1993) Pharyngography after head and neck irradiation: differentiation of postirradiation edema from recurrent tumor. AJR 161: 1205–1208
6. MacDougall RH, Orr JA, Kerr G, Duncan W (1990) Fast neutron treatment for squamous cell carcinoma of the head and neck: final report of Edinburgh randomised trial. Br Med J 301: 1241–1242
7. Khan MY (1974) Radiation-induced changes in skeletal muscle: an electron microscopy study. J Neuropathol Exp Neurol 33: 42–57
8. Scherer E, Sack H (1989) Strahlentherapie – eine Einführung in die radiologische Onkologie. Thieme, Stuttgart, New York, pp 202–225, 318–331
9. Sovik E, Lien H, Tveit K (1993) Postirradiation changes in the pelvic wall. Acta Radiol 34: 573–576
10. Maier W, Beck C, Hinkelbein W, Richter B (1994) Eustachian tube function after therapy of hypopharynx and larynx carcinoma. Laryngol Rhinol Otol 73: 164–168 [in German]

11. Ohashi Y, Nakai Y, Esaki Y, Onoyama Y (1989) An experimental study of mucociliary pathology of the eustachian tube in otitis media with effusion induced by irradiation. Arch Otorhinolaryngol 246: 428–432
12. Stephens LC, Schultheiss T, Price R, Ang K, Peters L (1991) Radiation apoptosis of serous acinar cells of salivary and lacrimal glands. Cancer 67: 1539–1543
13. Franzen L, Funegard U, Sundström S, Gustafsson H, Danielsson A, Henriksson R (1991) Fractionated irradiation and early changes in salivary glands: different effects on potassium efflux, exocygotic amylase release and gland morphology. Lab Invest 64: 279–283
14. Henriksson R, Fröjd Ö, Gustafsson H, Johnasson S, Yi-Qing C, Franzen L (1994) Increase in mast cells and hyaluronic acid correlates to radiation-induced damage and loss of serous acinar cells in salivary glands: the parotid and submandibular glands differ in radiation sensitivity. Br J Cancer 69: 320–326
15. Nagler RM, Baum B, Fox P (1993) Effects of X irradiation on the function of rat salivary glands at 3 and 40 days. Radiat Res 136: 392–396
16. Vissink A, Gravenmade EJ, Ligeon EE, Konings W (1990) A functional and chemical study of radiation effects on rat parotid and submandibular/sublingual glands. Radiat Res 124: 159–265
17. Franzen L, Funegard U, Ericson T, Henriksson R (1992) Parotid gland function during and following radiotherapy of malignancies in the head and neck: a consecutive study of salivary flow and patient discomfort. Eur J Cancer 28: 457–462
18. Leslie MD, Dische S (1994) The early changes in salivary gland function during and after radiotherapy given for head and neck cancer. Radiother Oncol 30: 26–32
19. Knospe W, Bloom J, Crosby W (1966) Regeneration of locally irradiated bone marrow. Dose dependent, long-term changes in the rat, with particular emphasis upon the vascular and stromal reaction. Blood 28: 398–415
20. Aitasalo K (1986) Bone tissue response to irradiation and treatment model of mandibular irradiation injury. An experimental and clinical study. Acta Otolaryngol 428 (Suppl):1–54
21. Bedwinek JM, Shukovsky L, Fletcher G, Daley T (1976) Osteonecrosis in patients treated with definitive radiotherapy for squamous cell carcinomas of the oral cavity and naso- and oropharynx. Radiology 119: 665–667
22. Murray CG, Daly T, Zimmermann SO (1980) The relationship between dental desease and radiation necrosis of the mandible. Oral Surg 49: 99–104
23. Schratter-Sehn A-U, Handl-Zeller L, Strassl H, Braun O, Dobrowsky W (1991) Osteonecrosis of the mandibula after radiation/chemotherapy of neck tumors. Strahlenther Onkol 167: 165–168 [in German]
24. Bachmann G, Rössler R (1993) MRI in diagnosis of radiation induced mandibula osteonecrosis. Fortschr Röntgenstr 159: 347–354 [in German]
25. Kauczor H-U, Dietl B, Kreitner K-F, Brix G (1992) Bone marrow changes after irradiation. Radiologe 32: 516–522 [in German]
26. Dietl B, Kauczor H-U, Brix G, Semmler W, van Kaick G (1992) Late bone marrow changes in Hodgkin's disease patients: a characterization with proton chemical shift imaging. Eur Radiol 2: 20–24
27. Parmentier C, Morardet N, Tubiana M (1983) Late effects on human bone marrow after extended field radiotherapy. Int J Radiat Oncol Biol Phys 9: 1303–1309
28. Engelbrecht V, Pisar E, Fürst G, Mödder U (1995) Verlaufskontrolle und Rezidivdiagnostik maligner Kopf- und Halstumoren nach Radiochemotherapie. Vergleich zwischen Computertomographie und Kernspintomographie. Fortschr Röntgenstr 162: 304–310
29. Wagner-Manslau C, Lukas P, Herzog M, Kau R, Becker K (1994) MRI and proton-NMR relaxation times in diagnosis and therapeutic monitoring of squamous cell carcinoma. Eur Radiol 4: 314–323
30. Som PM, Urken ML, Biller H, Lidov M (1993) Imaging the postoperative neck. Radiology 187: 593–603
31. Sugimura K, Kuroda S, Furukawa T, Matsuda S, Yoshimura Y, Ishida T (1992) Tongue cancer treated with irradiation: assessment with MR imaging. Clin Radiol 46: 243–247
32. UICC TNM classification of malignant tumors, 4th edn. (1998) Hermanek Phutter RVP, Sobin LH, Wagner G, Wittekind C (eds). Springer, New York